Mechanism for Nucleotide Exchange in Monomeric Actin[†]

Carl Frieden* and Kalliopi Patane

Department of Biological Chemistry, Division of Biology and Biomedical Sciences, Washington University School of Medicine, St. Louis, Missouri 63110

Received July 20, 1987; Revised Manuscript Received January 19, 1988

ABSTRACT: Rabbit skeletal muscle G-actin has been treated to obtain ADP, $1,N^6$-ethenoadenosine diphosphate (ϵ-ADP), or $1,N^6$-ethenoadenosine triphosphate (ϵ-ATP) at the nucleotide binding site and either Mg^{2+} or Ca^{2+} at high- and moderate-affinity metal binding sites. Apparent rates or rate constants for the displacement of the actin-bound nucleotides by ϵ-ATP or ATP have been obtained by stopped-flow measurements at pH 8 and 20 °C of the fluorescence difference between bound and free ϵ-ATP or ϵ-ADP. In the presence of Ca^{2+}, displacement of ADP by ϵ-ATP or ϵ-ADP by ATP is a biphasic process, but in the presence of low (<10 μM) Mg^{2+} concentrations, it is a slow first-order process. At high levels of Mg^{2+} (>50 μM), low ADP concentrations displace ϵ-ATP from G-actin as a consequence of Mg^{2+} binding to moderate-affinity sites on the actin. Displacement of ϵ-ATP by ATP in the presence of either Ca^{2+} or Mg^{2+} is slow at low ATP concentrations, but the rate is increased by high ATP concentrations. Using ethylene glycol bis(β-aminoethyl ether)-N,N,N',N'-tetraacetic acid, we find that nucleotide exchange is affected differently by the removal of Ca^{2+} from the high-affinity site compared to Ca^{2+} removal from moderate-affinity sites. A mechanism for the displacement reaction is proposed in which there are two forms of an actin–ADP complex and metal binding influences the ratio of these forms as well as the binding of ATP. It is concluded that, in general, the presence of Ca^{2+} strengthens ATP binding relative to ADP, while the presence of Mg^{2+} weakens ATP binding relative to ADP.

Monomeric actin contains a tightly bound molecule of ATP (Straub & Feuer, 1950) that is hydrolyzed to ADP during polymerization (Oosawa & Kasai, 1971). The hydrolysis reaction is considered to be important (Korn, 1982; Frieden, 1985) with respect to the rate of growth of the actin filaments, the critical concentration (defined as the concentration of monomer in equilibrium with polymer), the effect of cytochalasin D (Goddette & Frieden, 1986), the extent of treadmilling in an actin filament (due to differential rates of growth at the two ends of the filament) (Wegner, 1976), Mg^{2+}-induced conformational changes (Frieden et al., 1980; Frieden, 1982; Frieden & Patane, 1985), and possibly the extent of nuclei formation. Understanding the ATP–ADP exchange process is essential to understanding the role of the hydrolysis reaction. Thus, it is useful to study the exchange reaction of the monomer under a variety of conditions related to polymerization or depolymerization of actin.

The results of such a study may also serve as a basis for studying the exchange reaction when actin is complexed with various actin-binding proteins like gelsolin (Coue & Korn, 1986) or profilin (Nishida, 1985) as well as questions related to nucleotide-exchange reactions in subunits at the ends of filaments.

Although ^{14}C-labeled ATP was originally used to measure the kinetics of ATP exchange (Kuehl & Gergely, 1969), it was observed by Thames et al. (1974) that a fluorescent analogue of ATP, ϵ-ATP,[1] binds almost as tightly to monomeric actin as ATP itself and that, on binding, the fluorescence increases. This observation led to a number of studies on the exchange process in monomeric actin and particularly to the determination of ratios of dissociation constants for ADP, ATP, and ϵ-ATP (Neidl & Engel, 1979; Wanger & Wegner, 1983; Waechter, 1975; Waechter & Engel, 1975, 1977). Because

monomeric actin inactivates rapidly in the absence of nucleotides (Oosawa & Kasai, 1971), it is usually not possible to obtain absolute values for the dissociation constants for nucleotide binding, although some of the earlier studies estimated such values by measuring the rate at which ϵ-ATP is displaced by ATP or the rate at which ϵ-ATP displaces ADP. These latter studies, mostly performed in the presence of Ca^{2+}, were usually interpreted in terms of a simple displacement of ADP by ATP that could be affected by the presence of Ca^{2+} (Waechter & Engel, 1975). In the present paper we show that the exchange process in monomeric actin is more complex than usually assumed and is influenced by the presence of Ca^{2+} or Mg^{2+}, such that, in general, ATP binding relative to ADP binding is strengthened by Ca^{2+} and weakened by Mg^{2+}. However, there are different classes of metal binding sites (Zimmerle et al., 1987), and we show here that the exchange process is affected by the metal present in the tight binding site as well as in those sites of moderate affinity.

MATERIALS AND METHODS

Materials. Yeast hexokinase, ATP (99–100% pure), ADP, ϵ-ATP, and ϵ-ADP were obtained from Sigma. However, it was essential that the commercially available ADP be freed of ATP for the experiments reported here. Ron Harris, Sigma, kindly provided ADP as a ~30 mM solution containing ~1 M NaCl but essentially no ATP. This material was precipitated by the addition of ethanol and the precipitate dried for 2–3 h under vacuum. It was then dissolved in 2 mM Tris-HCl buffer, pH 8, and stored frozen. Using a Varian MicroPAK AX-5 HPLC ion-exchange column equilibrated and eluted at room temperature with 0.35 M potassium phosphate and 1.3

[1] Abbreviations: ϵ-ATP or ϵ-ADP, $1,N^6$-ethenoadenosine triphosphate or diphosphate; EGTA, ethylene glycol bis(β-aminoethyl ether)-N,N,N',N'-tetraacetic acid; DTE, dithioerythritol; Tris, tris(hydroxymethyl)aminomethane; Ap_5A, diadenosine 5'-pentaphosphate.

M NaCl, pH 3.5, we found that the material contained less than 0.004% ATP. $CaCl_2$ (Puratronic) and Ultrapure $MgSO_4$ were obtained from Ventron Corp., Alfa Division. All other materials used were of reagent grade, and all solutions were made with deionized distilled water.

Purification and Preparations of Proteins. Rabbit skeletal muscle G-actin was isolated and purified according to the procedure of Spudich and Watt (1971), modified (Frieden et al., 1980) with a Sephadex G-150 gel filtration step as described (MacLean-Fletcher & Pollard, 1980). Actin was stored at −20 °C after lyophilization in the presence of sucrose (2 mg of sucrose/mg of actin). Lyophilized actin was dissolved and dialyzed at 4 °C for 1–2 days against 2 mM Tris-HCl, pH 8, containing 200 μM ATP, 200 μM Ca^{2+}, 0.5 mM DTE, and 1.5 mM NaN_3. The protein concentration was determined spectrophotometrically by using $E^{1mg/mL} = 0.63$ at 290 nm (Houk & Ue, 1974) or by the method of Bradford (1976).

G-Actin containing Ca^{2+} and ADP was prepared as follows: Lyophilized actin was taken up in 2 mM Tris-HCl, pH 8, buffer containing 50 μM ATP, 200 μM Ca^{2+}, 0.5 mM DTE, and 1.5 mM NaN_3 and dialyzed overnight against this buffer at 5 °C. This actin (~2–3 mg/mL) was polymerized at room temperature in the presence of 2 mM Ca^{2+} and 20 mM Tris-HCl, pH 8. After polymerization was complete (approximately 30 min), the actin was centrifuged at 100000g for 1 h at 20 °C. The pellet was washed several times with 2 mM Tris-HCl buffer, pH 8, containing 50 μM ADP, 10 μM Ca^{2+}, 0.5 mM DTE, and 1.5 mM NaN_3, homogenized at 5 °C, and diluted 10-fold into the same buffer. The diluted actin was allowed to stand at 5 °C for 30 min and then rehomogenized to ensure complete depolymerization. It was then concentrated at 5 °C by centrifugation through Amicon Centriflo cones (CF25) to a concentration of 1–2 mg/mL. The procedure results in about a 20% loss of protein. The concentrated actin was centrifuged twice through small columns of Sephadex G-25 previously equilibrated with 2 mM Tris-HCl, pH 8, containing 50 μM ADP, 10 μM Ca^{2+}, 0.5 mM DTE, and 1.5 mM NaN_3. The Ca^{2+} concentration of the final actin solution was then raised to 50 μM to prevent inactivation. This actin solution was examined for Mg^{2+} content by atomic absorbance and found to contain less than 5–10% Mg^{2+}/mol of actin. G-Actin containing ADP prepared by modification of the procedure described by Pollard (1984) in which polymerization is induced by Mg^{2+} and hexokinase is used to deplete any free ATP results in higher levels of Mg^{2+} (up to 20–25% Mg^{2+}/mol of actin). Selden et al. (1987), for example, report that actin containing ADP prepared by using hexokinase contained about 20% Mg^{2+}.

G-Actin containing Mg^{2+} and ADP was prepared as follows: Actin was polymerized (room temperature) at a concentration of 2 mg/mL in G buffer (2 mM Tris-HCl, pH 8.0, 200 μM ATP, 200 μM Ca^{2+}, 0.5 mM DTE, and 1.5 mM NaN_3) with the addition of 2 mM Mg^{2+}. Yeast hexokinase (0.01 mg/mL), glucose (200 μM), and diadenosine 5′-pentaphosphate (Ap₅A), a potent inhibitor of myokinase (10 μM), were added, and the actin solution was left at room temperature for 10–15 min. The solution was diluted 10-fold in ADP–G buffer (2 mM Tris-HCl, pH 8, 50 μM Mg^{2+}, 50 μM ADP, 0.5 mM DTE, and 1.5 mM NaN_3), passed twice through a 22-gauge syringe needle, and allowed to stand for 15–20 min to complete depolymerization. The diluted actin was concentrated at 5 °C by centrifugation through Amicon Centriflo cones (CF25) to a concentration of 1–2 mg/mL, which resulted in about a 20% loss of protein. At this point, the actin solution contained 2 mM Tris-HCl, pH 8.0, ~50 μM ADP, ~20 μM glucose

6-phosphate, 0.2 mM Mg^{2+}, some hexokinase, and 1.5 mM NaN_3. The concentrated actin was centrifuged twice through small columns of Sephadex G-25 previously equilibrated with 2 mM Tris-HCl, pH 8.0, containing 50 μM ADP, 50 μM Mg^{2+}, 0.5 mM DTE, and 1.5 mM NaN_3. This step removed most of the remaining glucose and hexokinase. The concentrations of glucose and hexokinase were further reduced (>10-fold) by the dilution factor of the stock ADP actin for our experiments. Actin containing ADP was prepared fresh each day and stored on ice.

The Ca^{2+} content of actin so prepared was assayed by using Quin 2 (Tsien, 1980) in the presence of 0.15 mM Mg^{2+} as described by Zimmerle et al. (1987). Any tightly bound Ca^{2+} is displaced by this method and detected by the fluorescence change associated with Ca^{2+} binding to Quin 2. No Ca^{2+} was observed in these preparations.

Actin containing ε-ADP was prepared by first obtaining actin containing ADP in the presence of Ca^{2+} as described above. ε-ATP was then added to a final concentration slightly larger than the actin concentration and the solution allowed to stand at room temperature for 10–15 min. The solution was centrifuged twice through small Sephadex G-25 columns preequilibrated with 2 mM Tris-HCl, pH 8, containing 50 μM ε-ATP, 50 μM Ca^{2+}, 0.5 mM DTE, and 1.5 mM NaN_3. Depending on the cation content of the final product, actin was then processed as follows: If actin was to contain Ca^{2+}, the actin with ε-ATP was polymerized by the additions of 20 mM Tris-HCl, pH 8, and 2 mM $CaCl_2$ and left at 4 °C overnight. It was then centrifuged and the pellet homogenized and then diluted 10-fold in buffer containing 2 mM Tris-HCl, 10 μM Ca^{2+}, and 50 μM ε-ADP at pH 8. This material was then concentrated by using Amicon Centriflo cones (CF25) and again centrifuged through small Sephadex G-25 columns that had been previously equilibrated with Ca^{2+} and ε-ADP. The Ca^{2+} concentration of the final actin solution was raised to 50 μM to prevent inactivation.

If the actin was to contain Mg^{2+}, the actin with ε-ATP was polymerized by the addition of 2 mM Mg^{2+} and left at 4 °C overnight. It was then depolymerized in the presence of hexokinase (0.01 mg/mL), glucose (200 μM), and Ap₅A (10 μM) by passing it twice through a 22-gauge syringe needle. This material was diluted 10-fold in buffer containing 2 mM Tris-HCl, 50 μM Mg^{2+}, and 50 μM ε-ADP at pH 8. This material was then concentrated by using Amicon Centriflo cones (CF25) and again centrifuged through small Sephadex G-25 columns that had been previously equilibrated with Mg^{2+} and ε-ADP. Once prepared, either actin was used in experiments as quickly as possible (within several hours).

Methods. Fluorescence stopped-flow experiments were obtained by using a Durrum stopped-flow apparatus in the fluorescence mode and a Schott GG385 filter on the emission side to filter out the excitation wavelength (335 nm). The fluorescence coefficient for ε-ATP bound to actin, $X_{\epsilon A}$, was calculated from the expression

$$\frac{F_t - F_b - X_\epsilon(\epsilon_t - \epsilon A)}{\epsilon A}$$

where F_t is the total fluorescence after ε-ATP addition, F_b is the background (buffer) fluorescence, X_ϵ is the fluorescence coefficient for free ε-ATP (determined from separate experiments), ϵ_t is the total ε-ATP concentration, and ϵA is the total actin concentration containing ε-ATP. The ratio $X_{\epsilon A}/X_\epsilon$ was 2–3-fold under our conditions, and the specific values of $X_{\epsilon A}$ and X_ϵ determined were used in simulation of the full time course of the experimental data using the program KINSIM (Barshop et al., 1983) and a more recently developed program

FITSIM, which allows nonlinear fitting of rate constants to several progress curves simultaneously for a given mechanism (Zimmerle et al., 1987).

Biphasic progress curves were also analyzed by a two-exponential fitting program for which the equation used is that for two consecutive first-order reactions and is of the form

$$Be^{-k_1 t} + (1 - B)e^{-k_2 t}$$

where B is the extent of the fast phase and k_1 and k_2 are the rate constants for the fast and slow phases, respectively.

Fluorescence titration curves using ε-ATP were performed with a SPEX fluorometer (350 and 410 nm for excitation and emission wavelengths, respectively) in an E/R mode to correct for any fluctuations of the excitation intensity.

It is essential for the interpretation of the results that we obtain accurate values for the dissociation constants for metal binding to ATP under the same conditions used for the nucleotide-exchange experiments. Dissociation constants for ATP binding to Ca^{2+} and Mg^{2+} were determined at 20 °C, pH 8, in 2 mM Tris-HCl buffer. We determined these constants by titrating from 10–50 μM concentrations of ATP with varying concentrations of Ca^{2+} and measuring the free Ca^{2+} concentration by changes in the absorbance difference (550–480 nm) of tetramethylmurexide (0.00176/μM Ca^{2+}). From the free and total concentrations, the dissociation constant can be calculated. The dissociation constant for Ca^{2+} binding to the tetramethylmurexide, determined separately, is so high (1.34 mM) that the formation of the Ca^{2+}–tetramethylmurexide complex does not perturb the Ca^{2+}–ATP equilibrium. The dissociation constant for the Mg^{2+}–ATP complex was evaluated by competition experiments between Ca^{2+} and Mg^{2+} by using the Ca^{2+}–ATP dissociation constant determined. The values for the Ca^{2+}–ATP and Mg^{2+}–ATP dissociation constants determined by this method were found to be 5 and 3 μM, respectively, under these conditions and very close to those used previously (Frieden, 1982) by extrapolation of literature values to this ionic strength, temperature, and pH (6 and 3 μM for Ca^{2+} and Mg^{2+}, respectively). It was assumed that the dissociation constant for ε-ATP was the same as that for ATP.

RESULTS

Relative Binding Affinities of Nucleotides. Since the fluorescence of ε-ATP is enhanced on binding to G-actin (Thames et al., 1974), it is possible to determine ratios of dissociation constants by titrating G-actin containing ε-ATP with either ADP or ATP. Absolute values for these dissociation constants were not determined since nucleotide-free actin is quite unstable (Oosawa & Kasai, 1971). Relative dissociation constants were obtained from the titration data by using a program that solves the multiple equilibria involved in nucleotide binding to actin and to metal (Storer & Cornish-Bowden, 1976). In addition, the ratio of dissociation constants $K_{\epsilon\text{-ATP}}/K_{ADP}$ was obtained by titrating G-actin containing ADP with ε-ATP at several concentrations of ADP. These data were analyzed by using the previously described kinetic simulation program KINSIM (Barshop et al., 1983), which was modified to simulate titration curves. In these cases also, data analysis included the contribution of the metal–ATP or metal–ε-ATP complex.

Table I gives the ratio of dissociation constants obtained under different conditions. In the presence of Ca^{2+} or at low Mg^{2+} concentrations, ε-ATP binds about 5–10-fold less tightly than ATP. The ratio of the ADP to ε-ATP dissociation constant, however, depends markedly on the metal, ranging from about 100-fold at low Mg^{2+} concentration to 14000-fold

Table I: Ratios of Nucleotide Dissociation Constants to G-Actin[a]

conditions	$\dfrac{K_{\epsilon\text{-ATP}}}{K_{ATP}}$	$\dfrac{K_{ADP}}{K_{\epsilon\text{-ATP}}}$	$\dfrac{K_{ADP}}{K_{ATP}}$[b]
Ca–G-actin, $[Ca^{2+}] = 4$ μM	8	1200	9600
Ca–G-actin, $[Ca^{2+}] = 50$ μM	8	14000	120000
Mg–G-actin, $[Mg^{2+}] = 7$ μM	5	100	500
Mg–G-actin, $[Mg^{2+}] = 100$ μM		100	

[a] Determined at pH 8.0 in 2 mM Tris-HCl buffer at 20 °C containing 0.5 mM DTE and 1.5 mM NaN_3. Errors are ±10–20%. [b] Calculated from the first two columns.
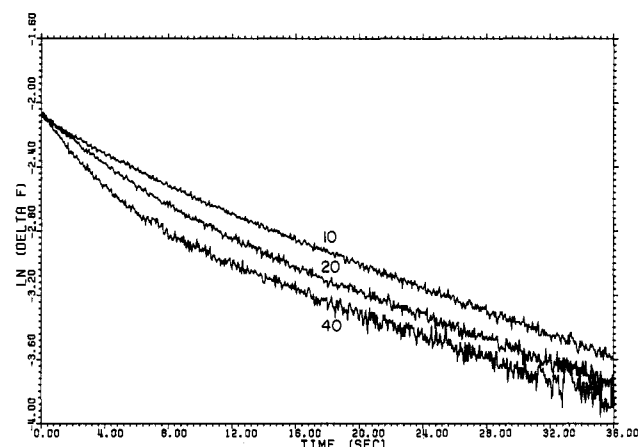

FIGURE 1: First-order plot of the fluorescence enhancement observed on addition of ε-ATP to G-actin containing ADP in the presence of 50 μM Ca^{2+} using the stopped-flow apparatus. Experiments were performed in 2 mM Tris-HCl, pH 8, 20 °C, 10 μM ADP, 0.5 mM DTE, and 1.5 mM NaN_3. The final G-actin concentration was 4 μM, and the ε-ATP concentrations (final) are as labeled.

at high Ca^{2+} concentration. This latter ratio is considerably larger than that of 30 observed by Neidl and Engel (1979). The ratio of dissociation constants is also dependent on the Ca^{2+} concentration, indicating that Ca^{2+} binding to moderate-affinity sites on actin ($K_d \sim 20$ μM; Zimmerle et al., 1987) can influence the relative binding of nucleotides. In addition, the data show that stoichiometric levels of ATP will completely displace any ε-ADP and most ε-ATP bound to actin.

Addition of ε-ATP to ADP–G-Actin in the Presence of Ca^{2+}. The fluorescence change associated with ε-ATP addition to G-actin containing ADP can be followed by using stopped-flow methods. In the presence of Ca^{2+}, this fluorescence change is biphasic. Apparent rate constants and extents for the two phases can be determined from these curves by using a two-exponential fitting program that analyzes the data in terms of consecutive first-order reactions (Methods). At high Ca^{2+} concentrations both the apparent rate constant and the extent of the fast phase depend upon the ε-ATP and Ca^{2+} concentration as well as the ADP concentration. On the other hand, the apparent rate constant for the slow phase is relatively independent of the concentration of these ligands. As an illustration, Figure 1 shows a first-order plot of stopped-flow data observed on addition of ε-ATP concentration (10–40 μM) to 4 μM G-actin containing ADP at a given total concentration of Ca^{2+} (50 μM) and ADP (10 μM). Values of these apparent rate constants and the extent of the fast phase are given in Table II. In the experiment shown in Figure 1, the concentration of free ε-ATP is considerably less than the total concentration due to metal–nucleotide complex formation. Thus, by use of a K_d for the ε-ATP–Ca^{2+} complex of 5 μM (see Methods), the free ε-ATP concentrations are 1.1, 2.6, and 8.5 μM for total concentrations of 10, 20, and 40 μM, respectively.

Interpretation of the data such as those given in Figure 1 is complicated by the low level of free ε-ATP as well as by

Table II: Apparent Rate Constants for ϵ-ATP Addition to ADP–G-Actin[a,b]

[ϵ-ATP] (μM)	0[c] Ca^{2+}			5 μM Ca^{2+}			50 μM Ca^{2+}		
	k_1 (s^{-1})	k_2 (s^{-1})	% fast phase	k_1 (s^{-1})	k_2 (s^{-1})	% fast phase	k_1	k_2	% fast phase
5	0.91	0.045	78	0.38	0.04	59	0.10	0.035	43
10	0.99	0.043	77	0.58	0.036	65	0.12	0.036	68
20	1.04	0.038	77	0.94	0.037	67	0.18	0.042	81
40	1.26	0.035	76	1.28	0.025	68	0.33	0.035	85

[a] Determined in 2 mM Tris-HCl, pH 8.0, 20 °C, in the presence of 10 μM ADP, 0.5 mM DTE, 1.5 mM NaN$_3$, and G-actin containing ADP. [b] Data analyzed by a two-exponential fitting program assuming sequential first-order reactions (see Methods). [c] EGTA (100 μM) added simultaneously with ϵ-ATP (see text).

changes in the free Ca^{2+} and Ca^{2+}–ϵ-ATP concentration. With respect to the latter, we assume that the complex Ca^{2+}–ϵ-ATP does not bind to actin. This assumption is based on several observations. First, the charge of the nucleotide is decreased in the complex; second, the structure of the metal complex is quite different from that of the free nucleotide; third, free ATP clearly binds tightly; and, finally, no relationships that are to be developed here appear to depend on the complex concentration as opposed to the free Ca^{2+} or ATP concentration. However, the data analysis always includes the formation of any metal–nucleotide complex when the free ATP or ϵ-ATP concentration is calculated.

One way to diminish the complication due to the Ca^{2+}–nucleotide complex is to perform experiments at low Ca^{2+} concentration or to add EGTA simultaneously with the ϵ-ATP to give zero (or very low) Ca^{2+} levels (EGTA experiments are discussed later). When the Ca^{2+} concentration is kept at levels lower than the ϵ-ATP concentration, the extent of the two phases is independent of the ϵ-ATP concentration, although the apparent rate constant for the fast phase is somewhat dependent on the ϵ-ATP concentration (Table II). It should be noted, however, that the apparent rate constant for the fast phase does not change in direct proportion to the ϵ-ATP level, and at zero levels, the apparent rate constant is almost independent of the ϵ-ATP concentration. This means that a binding step (e.g., actin + ϵ-ATP) cannot be one of the observed phases of the fluorescence change since there is not a direct dependence of the rate constant on ϵ-ATP concentration. Apparent rate constants determined by a two-exponential fit at zero, high, and low Ca^{2+} concentrations are shown in Table II. The data show that as the Ca^{2+} concentration increases from 5 to 50 μM, at any given ϵ-ATP level, the apparent rate constant for the fast phase becomes smaller. At 50 μM Ca^{2+}, the extent of the fast phase relative to the total change increases as the ϵ-ATP concentration increases.

The experiments described in Figure 1 and Table II were performed without regard to the free concentrations of Ca^{2+} and ϵ-ATP but rather at given total concentrations. Figure 2 shows a series of experiments in which the free ϵ-ATP concentration was held constant (20 μM) and data were obtained as a function of the free Ca^{2+} concentration. The free concentrations of Ca^{2+} and ϵ-ATP were calculated from the total concentrations by using a dissociation constant of 5 μM for the Ca–ϵ-ATP complex (see Methods). These data show that as the free Ca^{2+} concentration increases, the extent of the fast phase increases, although the initial rate of this phase is the same. The data illustrate some of the difficulties in interpretation because, although the initial rates are the same, the apparent rate constants for the fast phase decrease as the free Ca^{2+} concentration increases. This result is mostly due to a change in the extent of the fast phase relative to the total change. The interpretation of these data is given later, but it should be noted that the levels of Ca^{2+} which affect the extent of the fast phase are in the micromolar range, consistent with the presence of Ca^{2+}-binding sites of moderate affinity
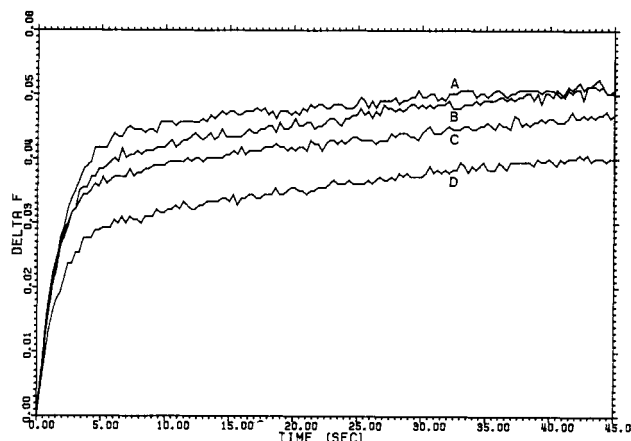

FIGURE 2: Fluorescence enhancement (arbitrary units) observed on addition of ϵ-ATP to 4 μM G-actin containing ADP at constant free ϵ-ATP concentration. Stopped-flow experiments were performed in 2 mM Tris-HCl, pH 8, 20 °C, 10 μM ADP, 0.5 mM DTE, and 1.5 mM NaN$_3$. Use of a dissociation constant of 5 μM for the Ca–ϵ-ATP complex (see Materials and Methods) yielded free ϵ-ATP concentrations of 20 μM in all experiments, and the free Ca^{2+} concentrations were 10 (A), 6 (B), 4 (C), and 2 μM (D).
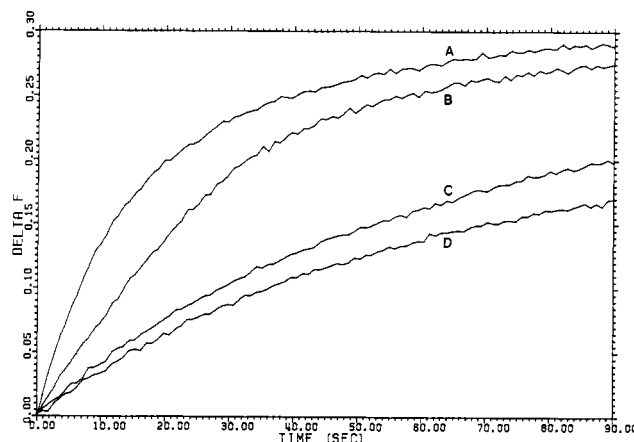

FIGURE 3: Fluorescence enhancement (arbitrary units) observed on addition of 20 μM ϵ-ATP to 4 μM G-actin at different ADP concentrations. Stopped-flow experiments were performed in 2 mM Tris-HCl, pH 8, 20 °C, containing 50 μM Ca^{2+}, 0.5 mM DTE, and 1.5 mM NaN$_3$. The experiments were performed with the actin incubated with 10 μM ADP (A), 100 μM ADP (B), 500 μM ADP (C), or 1000 μM ADP (D) (final concentrations) added with the ϵ-ATP.

(Zimmerle & Frieden, 1986; Zimmerle et al., 1987; Frieden et al., 1980). The effect of removing Ca^{2+} from the very tight binding site (K_d <0.05 μM) will also be described later.

Figure 3 shows the effect of increasing ADP concentration on addition of ϵ-ATP to G-actin containing ADP. The effect of high levels of ADP is about as inhibitory as expected from the ratio of dissociation constants shown in Table I. Further, the data can be fit by using the mechanism shown in eq 3 and 4 (see Discussion).
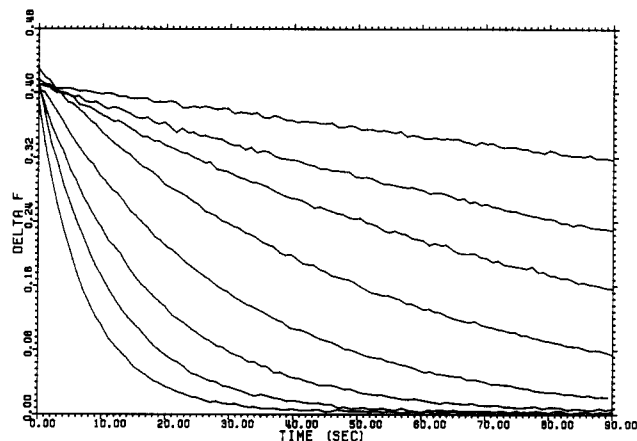
FIGURE 4: Fluorescence decrease (arbitrary units) observed on addition of ATP to G-actin containing ϵ-ATP (4 μM). Stopped-flow experiments performed in 2 mM Tris-HCl, pH 8, 20 °C, in the presence of 10 μM ADP, 10 μM Ca^{2+}, 0.5 mM DTE, 1.5 mM NaN$_3$, and 1 μM free ϵ-ATP. The ATP concentrations used were, from top to bottom, 20 μM, 60 μM, 110 μM, 250 μM, 500 μM, 1 mM, 2 mM, and 4 mM.

Addition of ATP to G-Actin Containing ϵ-ATP in the Presence of Ca^{2+}. Since ATP is bound to G-actin more tightly than ϵ-ATP (Table I), ϵ-ATP can be almost completely displaced by stoichiometric concentrations of ATP. At low ATP concentrations (<50 μM), the displacement is not exactly first order, but the major portion of the curve has an apparent rate constant of 0.003–0.006 s^{-1}, and this value does not vary greatly with Ca^{2+} concentration. However, as has been previously observed by both Kuehl and Gergely (1969) and Waechter and Engel (1975), the rate of ϵ-ATP displacement is a function of the ATP concentration. Figure 4 shows stopped-flow experiments as a function of ATP concentration at low Ca^{2+} and ADP concentrations (10 μM each). Above about 100 μM ATP, the displacement process is strictly first order. At the highest ATP level used (4 mM), the rate constant has markedly increased to about 0.15 s^{-1}. Similar, but not identical, results are observed at higher Ca^{2+} concentrations (data not shown). From a double-reciprocal plot of these data (not shown), it is found that the rate for displacement is reasonably constant at lower ATP levels but that, at very high ATP concentrations (>1 mM), the apparent rate constant for the displacement reaction increases markedly. Extrapolation of this portion of the curve gives an apparent dissociation constant of about 5 mM and a maximum rate constant of about 0.25 s^{-1}. The effect does not appear to be due to changes in ionic strength since at lower ATP concentrations the addition of 0.1 M KCl only increases the rate by about 2-fold. While high ATP concentrations will certainly remove any Ca^{2+} from the moderate-affinity sites, such concentrations do not remove appreciable Ca^{2+} from the high-affinity site if the dissociation constant for that site is <0.05 μM (Estes et al., 1987; Gersham et al., 1986; Carlier et al., 1986; Konno & Morales, 1985).

When EGTA is preincubated with actin, thus removing Ca^{2+} from the high-affinity site (discussed below), the results are somewhat different. In this case the rate at low ATP levels increases only about 3-fold at 4 mM ATP (data not shown). Thus, the much larger increase observed in Figure 4 may reflect some other effect of ATP itself, such as ATP binding to a distinct site.

Effect of Mg^{2+}. While there is good evidence (Zimmerle et al., 1987; Gershman et al., 1986; Carlier et al., 1986; Konno & Morales, 1985) that G-actin contains one tight binding Ca^{2+} site (K_d <0.05 μM) and several moderate-affinity sites (K_d
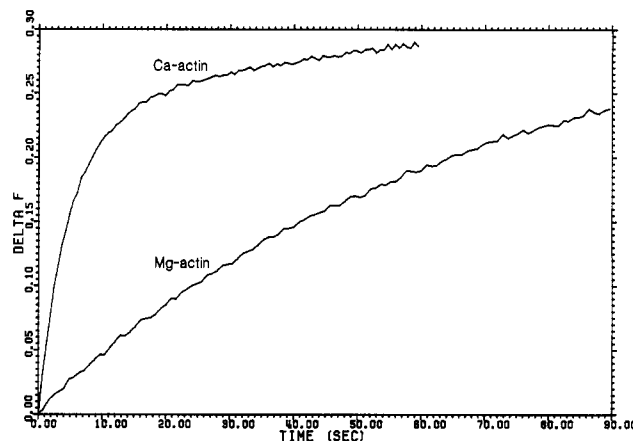
FIGURE 5: Fluorescence enhancement (arbitrary units) on addition of 10 μM ϵ-ATP to 4 μM G-actin containing ADP and tightly bound Ca^{2+} or Mg^{2+}. Stopped-flow experiments performed in 2 mM Tris-HCl, pH 8, 20 °C, 0.5 mM DTE, 1.5 mM NaN$_3$, and 10 μM ADP. For the Ca–actin experiment, the Ca^{2+} concentration was 12 μM, and for the Mg–actin experiment, the Mg^{2+} concentration was also 12 μM. The Mg–actin was prepared as described under Materials and Methods.
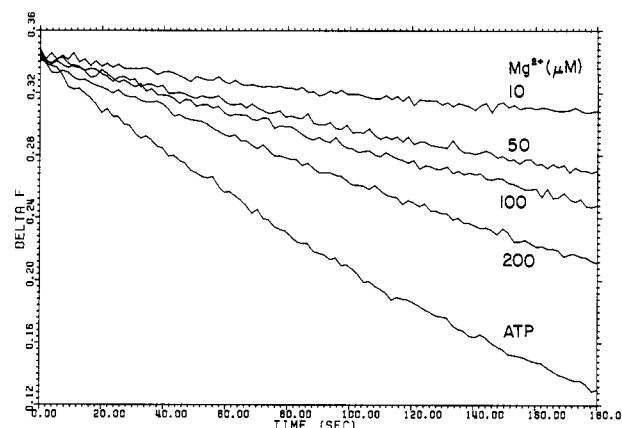

FIGURE 6: Fluorescence decrease (arbitrary units) following addition of Mg^{2+} to 4 μM G-actin containing ϵ-ATP. Stopped-flow experiments performed in 2 mM Tris-HCl, pH 8, 20 °C, 10 μM ADP, 0.5 mM DTE, 1.5 mM NaN$_3$, and 10 μM Ca^{2+}. Mg^{2+} concentrations are as indicated in the figure. Curve labeled ATP is that observed on addition of 50 μM ATP in the absence of Mg^{2+}.

$\sim$20 μM; Zimmerle et al., 1987), G-actin can also be prepared in which the tight binding Ca^{2+} has been replaced by Mg^{2+} (Zimmerle et al., 1987).

When ϵ-ATP is added to ADP–actin containing Mg^{2+} at the tight binding site and in buffer containing low (10 μM) Mg^{2+}, the results are quite different from those observed in the presence of Ca^{2+}. Figure 5 shows such an experiment, and it may be seen that instead of the two phases observed in the presence of Ca^{2+} only a single slow phase is observed with Mg–actin. The apparent rate constant for this single phase ($\sim$0.015 s^{-1}) is somewhat slower than that for the slow phase observed on displacing ADP with ϵ-ATP when Ca^{2+} is bound at the high-affinity site ($\sim$0.03 s^{-1}). This shifting from two phases to a single phase will be discussed later (Discussion) in terms of shifting the equilibrium between two actin forms that contain ADP.

At high Mg^{2+} concentrations, and in the presence of 10 μM ADP, very little added ϵ-ATP is incorporated into the Mg–actin. In fact, at higher Mg^{2+} levels ADP displaces ϵ-ATP even in the presence of low Ca^{2+} (where the tight binding site would contain Ca^{2+}). Figure 6 shows that, as a function of the Mg^{2+} concentration, there is a decrease in fluorescence, indicating release of ϵ-ATP from actin containing ϵ-ATP.

Table III: Rate Constants for Displacement of ε-ADP from G-Actin by 50 μM ATP[a,b]

conditions	k_1 (s^{-1})	k_2 (s^{-1})	% fast phase
50 μM Ca^{2+}	1.1	0.02	65
10 μM Ca^{2+}	1.45	0.034	40
18 μM Mg^{2+}		0.075	0
10 μM Mg^{2+}, actin preincubated with EGTA		0.045	0

[a] Determined in 2 mM Tris-HCl, pH 8.0 and 20 °C, 0.5 mM DTE, and 1.5 mM NaN$_3$ by using 4 μM G-actin. Experiments performed with Mg^{2+} using Mg^{2+}–actin prepared as described under Materials and Methods. [b] Data analyzed by a two-exponential fitting program assuming sequential first-order reactions.

Under these conditions (10 μM Ca^{2+}), the Mg^{2+} does not displace Ca^{2+} from the high-affinity site. The data are not consistent with the idea that Mg^{2+} is removing ε-ATP solely by chelation since, for example, Ca^{2+} at much higher concentrations does not remove ε-ATP from actin. Rather, the release of ε-ATP must be due to Mg^{2+} binding to moderate-affinity sites with a subsequent weakening of ε-ATP binding. Analysis of these data indicates that the apparent rate constant increases slightly and that nucleotide release is about 50% complete at 200 μM Mg^{2+}. Even at this Mg^{2+} concentration, the apparent rate constant is still quite low (0.006 s^{-1}) and is similar to that observed for the displacement of ε-ATP by low concentrations of ATP in the presence of Ca^{2+} (Figure 6, lowest curve). The interpretation of the apparent rate constant for ε-ATP removal by Mg^{2+} is complex, however, because high levels of Mg^{2+} induce a conformational change that is dependent on the presence of ATP (Frieden, 1982; Frieden & Patane, 1985). This conformational change probably occurs more rapidly than does the ADP displacement of ε-ATP caused by Mg^{2+}. It should also be noted that since ATP binds about 10 times more tightly than ε-ATP, Mg^{2+} release of ATP may be much slower than release of ε-ATP.

Observations similar to those shown in Figure 6 are made when Mg^{2+} is bound to the tight site. In this case, high Mg^{2+} concentrations are somewhat less effective in removing the ε-ATP than when Ca^{2+} is bound to the tight site (data not shown), but the results are still not consistent with removal by simple chelation of the Mg^{2+} with ε-ATP.

Displacement of ε-ADP from Actin. When ε-ADP bound to G-actin (see Methods for preparation) is displaced by ADP or ATP in the presence of Ca^{2+}, the displacement process is biphasic. The biphasic nature of ε-ADP displacement by ATP or the ADP displacement by ε-ATP suggests the same steps may be involved in both processes. Table III gives the apparent rate constants and the extent of the fast phase under different conditions of ε-ADP displacement. The apparent rate constants, in the presence of Ca^{2+}, are similar to those observed for the apparent rate constants for ε-ATP addition to G-actin containing ADP (Table II). As with those experiments the apparent rate constant for the fast phase shows a slight dependence on the free ATP concentration, while that for the slow phase appears similar in both types of experiments.

Displacement of ε-ADP by ADP or ATP using actin that contains Mg^{2+} in the tight binding site yields a different result. In this case, there is only a single slow phase ($k = \sim 0.045–0.075$ s^{-1}). This observation is similar to the displacement of ADP by ε-ATP in the presence of Mg^{2+}, in which there is also only a single slow phase.

Effect of EGTA. Many investigators have used EGTA to remove Ca^{2+} from solution as well as from actin itself. It was of interest, therefore, to examine the effect of EGTA on nucleotide exchange in relation to the occupation of the different
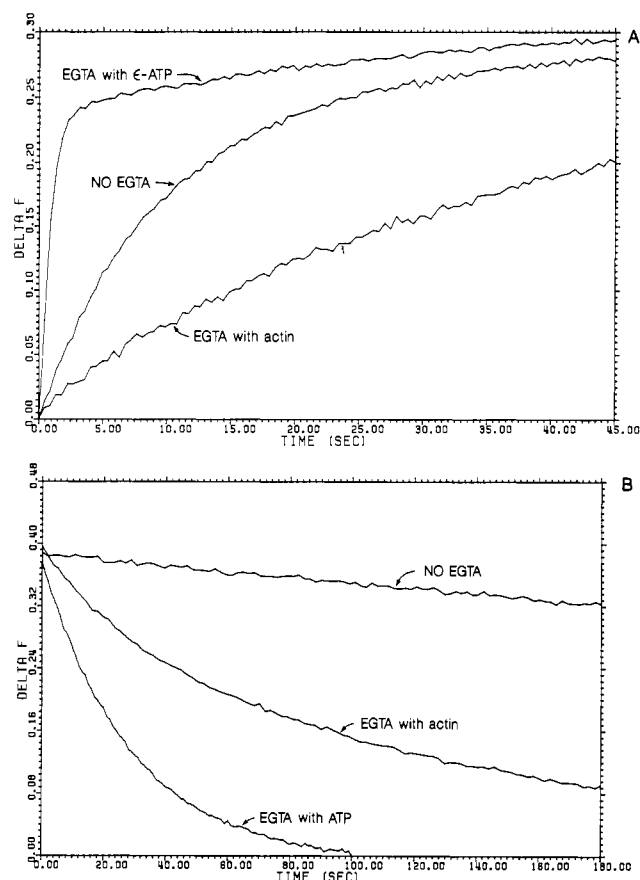

FIGURE 7: Fluorescence changes (arbitrary units) on addition of (A) 10 μM ε-ATP to G-actin containing ADP or (B) 20 μM ATP to G-actin containing ε-ATP. Stopped-flow experiments performed in 2 mM Tris-HCl, pH 8, 20 °C, 50 μM Ca^{2+}, 0.5 mM DTE, 1.5 mM NaN$_3$, and 10 μM ADP. In this figure, the control experiment is labeled "No EGTA". Experiments in which 100 μM EGTA is preincubated with the actin for 5 min prior to nucleotide addition are labeled "EGTA with actin". Those in which EGTA and nucleotide actin are labeled "EGTA with ε-ATP" (A) or "EGTA with ATP" (B).

classes of Ca^{2+}-binding sites (high and moderate affinity) that we have described previously (Zimmerle et al., 1987). Thus, stopped-flow experiments in the presence of a Ca^{2+} chelator like EGTA can be performed either by preincubating the actin with the chelator or by simultaneous addition of chelator with the displacing nucleotide to actin containing tightly bound Ca^{2+}. Addition of EGTA simultaneously with the displacing nucleotide will immediately remove all the free Ca^{2+} from moderate-affinity sites and only slowly remove the tightly bound Ca^{2+}. Since the half-time for removal of the tightly bound Ca^{2+} by chelator is on the order of 5–10 s (Zimmerle et al., 1987; Estes et al., 1987; Carlier et al., 1986), when actin is preincubated for about 5 min, all tightly bound Ca^{2+} should be removed as well. Figure 7A shows results for the addition of 10 μM ε-ATP to actin containing ADP in the absence of EGTA or when EGTA is preincubated with actin or when EGTA is added simultaneously with the ε-ATP. The results are strikingly different for these three experiments. When EGTA is added simultaneously with ε-ATP, there are two phases, but the apparent rate constant for the fast phase is almost 10 times faster than the control (1.13 vs 0.12 s^{-1} in 50 μM Ca^{2+}) and the extent somewhat larger. The rate constant for the slow phase (~ 0.03 s^{-1}) is about the same as in the control. Although the interpretation of this experiment is complicated by the simultaneous removal of Ca^{2+} from the tight binding site, the fast phase is probably rapid enough ($t_{1/2} < 1$ s) so that it occurs while Ca^{2+} is still at the tight binding

site. In contrast to the above experiment, when EGTA is preincubated with the actin, the fast phase disappears completely and the rate appears to be first order with a rate constant about the same as the usual slow phase ($k = \sim 0.03$ s^{-1}). Preincubation of G-actin containing ADP with EGTA leads to rather rapid inactivation presumably as a consequence of the Ca^{2+} being removed from the tight binding site. In this case, stopped-flow experiments were performed as rapidly as possible after EGTA was added to the actin (within 5 min). However, experiments at longer times gave the same results, although the extent of the fluorescence change was less as a consequence of the inactivation. G-Actin containing ATP or ϵ-ATP did not inactivate nearly so rapidly in the presence of EGTA.

Different results are also observed when low levels of ATP are used to displace ϵ-ATP in the presence or absence of EGTA. Figure 7B shows the displacement of ϵ-ATP by 20 μM ATP. As noted earlier, in the control experiment (50 μM Ca^{2+}, no EGTA) the displacement is not a first-order process. When actin is preincubated with EGTA, the rate constant is increased. However, when EGTA and ATP are added simultaneously, the rate increases even further. Again this latter experiment is complicated by the simultaneous removal of Ca^{2+} from the tight binding site. However, the data of Figure 7 clearly show that rates of nucleotide exchange clearly differ when Ca^{2+} is bound to the moderate- or high-affinity sites.

DISCUSSION

The results presented here indicate that nucleotide exchange in G-actin is not an easily described displacement process. It is dependent on metal ion and nucleotide concentration and is complicated by the fact that not only do nucleoside triphosphates bind metals, but actin itself contains at least two classes of metal-binding sites (Zimmerle et al., 1987) that influence the exchange process in different ways. Indeed, the effect of Ca^{2+} on the off rate of ATP has been pointed out by others (Kuehl & Gergely, 1969; Waechter & Engel, 1975; Waechter, 1975).

The following discussion will attempt to present a single mechanism that can explain the results.

The addition of ϵ-ATP to actin containing ADP is biphasic. When Neidl and Engel (1979) made this observation, they explained their data on the basis of eq 1 and 2, where A is

$$A + ADP \rightleftharpoons A \cdot ADP \qquad (1)$$

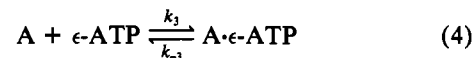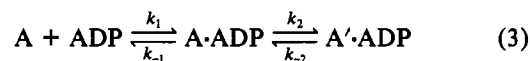$$A + \epsilon\text{-ATP} \rightleftharpoons A \cdot \epsilon\text{-ATP} \qquad (2)$$

G-actin. With this simple mechanism, they concluded that the slow phase corresponded to the off rate of ADP, while the fast phase was related to the addition of ϵ-ATP to the free actin. However, they had to assume that the on-rate constant for ADP was 3.6×10^{-4} M^{-1} s^{-1}, over 100-fold less than that for the ATP on-rate constant and for that expected from diffusion control. With this type of assumption, we also find it possible to fit the type of data shown in Figure 1. However, it is not possible to explain the biphasic curve we observe for the displacement of ϵ-ADP by ATP from actin using this commonly assumed mechanism (Table III). Nor is it likely that rate constants for addition of nucleotide to actin should differ markedly. Thus, this mechanism should be discarded.

Another simple mechanism is one in which there are two forms of free actin, A and A', only one of which (i.e., A) can bind nucleotide. In this case, the slow phase would be the conversion of the A' to A form of the actin. While such a mechanism can easily explain a biphasic process, a critical test is that the slow phase should disappear at nucleotide con-

centrations less than stoichiometric since in this case there would not be enough nucleotide to convert the A' form to A. Experiments designed with this test in mind show that both phases for ϵ-ATP addition to ADP-actin still occur even when the ϵ-ATP concentration is less than $^1/_5$ that of the actin concentration (data not shown). This result eliminates a scheme that assumes two forms of free actin.

Mechanisms that include two sequential first-order reactions to explain the observed biphasic data are those that involve a conformational change. Assuming the addition of ϵ-ATP is rapid, the following mechanism, where there are two forms of an actin–ADP complex, is suggested by the biphasic nature of ϵ-ADP or ADP displacement:

$$A + ADP \underset{k_{-1}}{\overset{k_1}{\rightleftharpoons}} A \cdot ADP \underset{k_{-2}}{\overset{k_2}{\rightleftharpoons}} A' \cdot ADP \qquad (3)$$

$$A + \epsilon\text{-ATP} \underset{k_{-3}}{\overset{k_3}{\rightleftharpoons}} A \cdot \epsilon\text{-ATP} \qquad (4)$$

Equations 3 and 4 are consistent with the displacement experiments shown in Figures 1 and 2 and Tables II and III that reflect two consecutive first-order reactions. In this mechanism, the extent of the fast phase reflects the amount of actin in the A·ADP form, and the apparent rate constant for this phase (k_{-1}) is its dissociation to A + ADP. The apparent rate constant for the slow phase (k_{-2}) is then the conversion of A'·ADP to A·ADP. Increasing concentrations of ADP would be expected to decrease the rate of the fast phase, and Figure 3 shows that this is indeed the case. Furthermore, the data in this figure are consistent with the ratio of dissociation constants for ϵ-ATP and ADP given in Table I.

As previously described (Zimmerle et al., 1987) actin contains different classes of metal-binding sites: one high-affinity site and several moderate-affinity sites. With the data presented here and utilizing the mechanism of eq 3 and 4, we can examine the effects of metal binding to these sites on nucleotide exchange.

The data can be fit by using this mechanism and assuming that Ca^{2+} binding to moderate-affinity sites alters the ratio A·ADP/A'·ADP as well as the rate constants k_{-1} and k_2. Taking into account Ca^{2+} binding to ϵ-ATP, the Ca^{2+} concentrations required to effect these changes are in the micromolar range and thus similar to values previously determined for Ca^{2+} binding to the moderate-affinity sites of actin (Zimmerle et al., 1987; Zimmerle & Frieden, 1986; Kuehl & Gergely, 1969; Waechter, 1975). Figure 7B shows that removal of Ca^{2+} from the moderate-affinity sites (simultaneous addition of EGTA and ϵ-ATP) increases the rate at which ϵ-ATP is displaced and thus presumably weakens ATP binding. We conclude, therefore, that Ca^{2+} binding to the moderate-affinity sites increases the amount of the A·ADP complex and strengthens ATP binding.

The data of Figure 6, in contrast, show that Mg^{2+} binding to the moderate-affinity sites weakens ϵ-ATP binding to such an extent that it is partially displaced even by low levels of ADP at 200 μM Mg^{2+}.

The removal of Ca^{2+} from the high-affinity site or the addition of Mg^{2+} to this site has different effects. Figure 7A shows that when Ca^{2+} is removed from the tight binding site (by preincubating actin with EGTA) or replaced by Mg^{2+} (Figure 5), there is only a single slow phase for ϵ-ATP addition. Thus, in terms of eq 3 and 4, all the actin must exist in the A'·ADP form under these conditions. With respect to ϵ-ATP binding, Figure 7B shows that removal of tightly bound Ca^{2+} increases the off rate but not to as great an extent as removing

Table IV: Divalent Cation Effects on Nucleotide Displacement[a]

site occupied		consequence	
tight	moderate	ADP displacement by ε-ATP	ε-ATP displacement by ATP
		slow, monophasic	increased relative to rate in presence of Ca^{2+} (see Figure 7B)
Ca^{2+}		biphasic	slow, depends markedly on ATP concentration (see Figure 4)
Ca^{2+}	Ca^{2+}	biphasic, affects A'·ADP/A·ADP ratio	slow, depends markedly on ATP concentration (see Figure 4)
Ca^{2+}	Mg^{2+}	slow, monophasic, but low ADP displaces ε-ATP	b
Mg^{2+}		slow, monophasic	depends somewhat on ATP concentration
Mg^{2+}	Mg^{2+}	slow, monophasic, but low ADP displaces ε-ATP	b

[a] Determined in 2 mM Tris-HCl, pH 8.0 at 20 °C, 0.5 mM DTE, and 1.5 mM NaN₃. [b] Experiment cannot be done since G-actin containing ε-ATP cannot be prepared at higher Mg^{2+} levels.

Ca^{2+} from the moderate-affinity sites. With actin containing Mg^{2+} at the tight binding site, the off-rate constant for ε-ATP displaced by 50 μM ATP is 0.016 s⁻¹, about 3-fold greater than with Ca^{2+} (~0.005 s⁻¹). Thus, Mg^{2+} binding or Ca^{2+} removal from the high-affinity site appears to weaken ε-ATP binding.

While it is clear from the above description that the effect of metal binding is complex, the data suggest, in general, that Ca^{2+} strengthens ATP binding relative to ADP, while Mg^{2+} weakens ATP binding relative to ADP. Conversely, ATP may strengthen Ca^{2+} binding relative to Mg^{2+}, and ADP may strengthen Mg^{2+} binding relative to Ca^{2+}. This latter result was recently obtained by Selden et al. (1987). The conclusion, however, is an oversimplification because it does not distinguish between the different classes of metal-binding sites. Table IV is an attempt to distinguish the effects of metal binding to high- and moderate-affinity sites and to describe the consequences of this binding on the nucleotide exchange reaction.

The data of Figure 4 are puzzling in that high levels of ATP do not give expected results. It appears that the nucleotide may bind at another low-affinity site which influences the rate at which it dissociates from the high-affinity nucleotide binding site. The observation with respect to ATP has been made previously (Kuehl & Gergely, 1969; Waechter & Engel, 1975).

Figure 6 shows that addition of Mg^{2+} will remove ε-ATP from G-actin even in the presence of Ca^{2+}. The apparent rate constant for the process is about 0.006 s⁻¹. Even if ATP is bound 5-10 times more tightly, then the half-time for ATP loss may be on the order of 10-20 min. Thus, during a slow polymerization process, a significant portion of the ATP might be removed from G-actin. Any free ADP might then bind since ADP binding is strengthened by the presence of Mg^{2+}. In fact, in the presence of an appreciable amount of ADP and Mg^{2+}, ATP may not exchange into G-actin.

Such a postulate might explain the time-dependent decrease in extent of polymerization sometimes observed in the polymerization process since G-actin containing ADP has a higher critical concentration than G-actin containing ATP (Lal et al., 1984; Pollard, 1984; Carlier et al., 1985). That ATP may not be able to exchange into G-actin in the presence of Mg^{2+} and high ADP concentrations was a conclusion also reached in our previous description of the effect of cytochalasin D on actin polymerization (Goddette & Frieden, 1986). In that model, we postulated that the cytochalasin stimulated hydrolysis of ATP and subsequent formation of G-actin containing ADP, as well as free ADP, accounted for the high critical concentrations observed in the presence of cytochalasin D. Finally, it has been suggested that most of the ADP contained within an actin filament does not exchange (Wang & Taylor, 1981) or exchanges very slowly (Brenner & Korn, 1984). The results presented here suggest that this may be simply a consequence of high Mg^{2+} levels and tighter ADP binding rather than a characteristic of the actin filament. The results, however, do not yet address the question of nucleotide exchange at the ends of actin filaments, an important point

relating to the extent of polymerization as well as the rate of growth and the issue of treadmilling (Wegner, 1976). Our results suggest, however, that such exchange may be dependent on Mg^{2+} and Ca^{2+} concentrations as well as any free ADP that may be present in the solution.

REFERENCES

Barshop, B. A., Wrenn, R. F., & Frieden, C. (1983) *Anal. Biochem. 130*, 134–145.

Bradford, M. M. (1976) *Anal. Biochem. 72*, 248–254.

Brenner, S. L., & Korn, E. D. (1984) *J. Biol. Chem. 259*, 1441–1446.

Carlier, M., Pantaloni, D., & Korn, E. D. (1985) *J. Biol. Chem. 260*, 6565–6571.

Carlier, M., Pantaloni, D., & Korn, E. (1986) *J. Biol. Chem. 261*, 10778–10792.

Coue, M., & Korn, E. D. (1986) *J. Biol. Chem. 261*, 1588–1593.

Estes, J. E., Selden, L. A., & Gershman, L. C. (1987) *J. Biol. Chem. 262*, 4952–4957.

Frieden, C. (1982) *J. Biol. Chem. 257*, 2882–2886.

Frieden, C. (1985) *Annu. Rev. Biophys. Biophys. Chem. 14*, 189–210.

Frieden, C., & Patane, K. (1985) *Biochemistry 24*, 4192–4196.

Frieden, C., Lieberman, D., & Gilbert, H. R. (1980) *J. Biol. Chem. 255*, 8991–8993.

Gershman, L. C., Selden, L. A., & Estes, J. E. (1986) *Biochem. Biophys. Res. Commun. 135*, 607–614.

Goddette, D. W., & Frieden, C. (1986) *J. Biol. Chem. 261*, 15974–15980.

Houk, T. W., Jr., & Ue, K. (1974) *Anal. Biochem. 57*, 453–459.

Konno, K., & Morales, M. (1985) *Proc. Natl. Acad. Sci. U.S.A. 82*, 7904–7908.

Korn, E. D. (1982) *Physiol. Rev. 62*, 672–737.

Kuehl, W. M., & Gergely, J. (1969) *J. Biol. Chem. 244*, 4720–4729.

Kwan, C., Erhard, K., & Davis, R. C. (1975) *J. Biol. Chem. 250*, 5951–5959.

Lal, A. A., Brenner, S. L., & Korn, E. D. (1984) *J. Biol. Chem. 259*, 13061–13065.

MacClean-Fletcher, S., & Pollard, T. D. (1980) *Biochem. Biophys. Res. Commun. 96*, 18–27.

Neidl, C., & Engel, J. (1979) *Eur. J. Biochem. 101*, 163–169.

Nishida, E. (1984) *Biochemistry 24*, 1160–1164.

Oosawa, F., & Kasai, M. (1971) in *Subunits in Biological Systems* (Timasheff, S. N., & Fasman, G. D., Eds.) pp 261–322, Dekker, New York.

Pollard, T. D. (1984) *J. Cell Biol. 99*, 769–777.

Selden, L. A., Gershman, L. C., Kinosian, H. J., & Estes, J. E. (1987) *FEBS Lett. 217*, 89–93.

Spudich, J. A., & Watt, S. (1971) *J. Biol. Chem. 246*, 4866–4871.

Storrer, A. C., & Cornish-Bowden, A. (1976) *Biochem. J. 159*, 1–5.

Straub, F., & Feuer, G. (1950) *Biochim. Biophys. Acta 4*, 455–470.

Thames, K. E., Cheung, H. C., & Harvey, S. C. (1974) *Biochem. Biophys. Res. Commun. 60*, 1252–1261.

Tsien, R. Y. (1980) *Biochemistry 19*, 2396–2404.

Waechter, F. (1975) *Hoppe-Seyler's Z. Physiol. Chem. 356*, 1821–1822.

Waechter, F., & Engel, J. (1975) *Eur. J. Biochem. 57*, 453–459.

Waechter, F., & Engel, J. (1977) *Eur. J. Biochem. 74*, 227–232.

Wang, Y.-L., & Taylor, D. L. (1981) *Proc. Natl. Acad. Sci. U.S.A. 78*, 5503–5507.

Wanger, M., & Wegner, A. (1983) *FEBS Lett. 162*, 112–116.

Wegner, A. (1976) *J. Mol. Biol. 108*, 139–150.

Zimmerle, C. T., & Frieden, C. (1986) *Biochemistry 25*, 4899–4906.

Zimmerle, C. T., Patane, K., & Frieden, C. (1987) *Biochemistry 26*, 6545–6552.

Substrate Specificities and Structure–Activity Relationships for the Nucleotidylation of Antibiotics Catalyzed by Aminoglycoside Nucleotidyltransferase 2″-I[†]

Cynthia A. Gates[‡] and Dexter B. Northrop*

Division of Pharmaceutical Biochemistry, School of Pharmacy, University of Wisconsin, Madison, Wisconsin 53706

Received August 13, 1987; Revised Manuscript Received January 15, 1988

ABSTRACT: Aminoglycoside nucleotidyltransferase 2″-I (formerly gentamicin adenylyltransferase) conveys antibiotic resistance to Gram-negative bacteria by transfer of AMP to the 2″-hydroxyl group of 4,6-substituted deoxystreptamine-containing aminoglycosides. The kinetic constants of thirteen aminoglycoside antibiotics and the magnesium chelates of eight nucleotide triphosphates were determined with purified enzyme. Eleven of the antibiotics exhibit substrate inhibition attributed to secondary binding of the aminoglycoside to an enzyme–AMP–aminoglycoside complex. Maximal velocities vary by only 4-fold, versus variation of values of V_{max}/K_m for the aminoglycosides of nearly 4000-fold, consistent with a Theorell–Chance kinetic mechanism as proposed for this enzyme [Gates, C. A., & Northrop, D. B. (1988) *Biochemistry* (second of three papers in this issue)] with the added specification that the binding of aminoglycosides is in rapid equilibrium. Under these conditions, V_{max}/K_m becomes k_{cat}/K_d, where k_{cat} is the net rate constant for catalysis (but not turnover) and K_d is the dissociation constant of aminoglycosides from a complex with enzyme and nucleotide. Values of k_{cat} fall closely together into three distinct sets, with the 3′,4′-dideoxygentamicins > gentamicins > kanamycins. These sets reflect unusual structure–activity correlations which are specific for catalysis but have nothing to do with the maximal velocity of this enzyme. The contribution of individual functional groups to binding was evaluated according to K_d values generated from substrate inhibition; specifically, binding is reduced by esterification at the 6″-carbon, hydroxylation of the 2′-carbon, unsaturation of the 4′,5′ carbon–carbon bond, methylation of the 6′-carbon or the 6′-amino groups, and ethylation of the 1-amino group. Comparisons between gentamicins and kanamycins are inconsistent with a common site of adenylylation at the 2″-hydroxyl but suggest either the 3′- or 4′-hydroxyl of the former. Unfortunately for the search for better antibiotics, most structure–activity relationships of enzymatic activity parallel antibiotic activity, with two exceptions being alkylation of the 1-amino group and stereochemical repositioning of the 5-hydroxyl group.

Aminoglycoside nucleotidyltransferase 2″-I [ANT(2″)-I][1] (EC 2.7.7.46) catalyzes the transfer of nucleotides to the 2″-hydroxyl group of 4,6-substituted deoxystreptamine-containing aminoglycoside antibiotics, accompanied by the release of pyrophosphate, according to the reaction:

$$\text{Mg–ATP} + \text{aminoglycoside} \rightarrow$$
$$\text{Mg–PP}_i + 2''\text{-AMP–aminoglycoside}$$
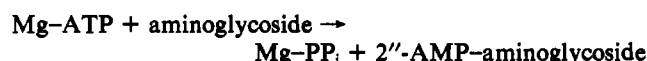
ANT(2″)-I was first identified as the biochemical basis for R factor mediated resistance to gentamicin by Benveniste and Davies (1971), who demonstrated a requirement for ATP in

---

[1] The enzyme was originally designated AAD(2″) by the plasmid nomenclature group, but the change to ANT(2″) was suggested since the nucleotide transferred to the antibiotic is not limited to adenine (Van Pelt & Northrop, 1984). The enzyme was further defined as ANT(2″)-I upon the discovery of a second aminoglycoside nucleotidyltransferase, designated ANT(2″)-II, with a different substrate range than that of ANT(2″)-I (Coombe & George, 1981).